ISBN: 978-3-95450-132-8 doi:10.18429/JACoW-IPAC2014-MOPRI018

INFLUENCE OF GROWTH METHOD ON K_3SB PHOTOCATHODE STRUCTURE AND PERFORMANCE*

S. G. Schubert, HZB, Berlin, Germany and BNL, Upton, USA
K. Attenkofer, J. Smedley, BNL, Upton, USA
T. Kamps, M. A. H. Schmeißer, HZB, Berlin, Germany
E. Muller, M. Ruiz-Oses, Stony Brook University, Stony Brook, USA
H. Padmore, J. Wong, LBNL, Berkeley, USA
J. Xie, ANL, Chicago, USA

Abstract

A combination of material science techniques is used to determine the influence of the growth parameters on structure and performance of photocathode materials. In-situ x-ray diffraction (XRD) and in-situ grazing incidence small angle x-ray scattering (GiSAXS), as well as after growth x-ray reflectivity (XRR) and $\theta/2\theta$ - XRD measurements were performed at synchrotron radiation sources. K_3Sb is a precursor material for the preparation of CsK_2Sb and Na_2KSb. The materials growth was studied intensively to optimize this intermediate growth step in terms of quantum efficiency and roughness. The results of two growth methods, a "layer by layer" type and a "super-lattice type", are presented, as well as the interaction of the K_3Sb phase with Cesium.

INTRODUCTION

Future high brightness photoelectron sources delivering >100 mA average current call for a new generation of photocathodes. Materials which qualify for this purpose should exhibit low intrinsic emittance, long lifetime and high quantum efficiency at photon energies in the visible range of the spectrum to relax drive laser requirements.
The Multi-Alkali-Antimonides are prime candidates to achieve these challenging objectives. These materials are long known and find application in photomultiplier tubes (PMT) [1]. Materials grown in the photomultiplier tube business usually show high quantum efficiency, but exhibit a rather rough surface which is unfavorable where low emittance is necessary [2, 3]
To address the stated material requirements a material science approach is applied. The crystal structure of the material is monitored in-situ which enables the identification of the compound composition and direct correlation to quantum efficiency. After growth performed XRR measurements provide a measure for surface roughness. In a nutshell the used setup enables the correlation between material composition, roughness, layer thickness and quantum efficiency.

* Work was supported by the US DOE, under Contracts DE-AC02-05CH11231, DE-AC02-98CH10886, KC0407-ALSJNT-I0013, DE-FG02-12ER41837 and DE-SC0005713 and German BMBF, Helmholtz-Association and Land Berlin. Use of CHESS is supported by NSF award DMR-0936384.

The focus of this study is the intermediate step in the production of CsK_2Sb, one of the prime candidates for the use as photocathode. Potassium and Antimony built up a variety of modifications [4]. The materials produced mainly consist of K_3Sb. K_3Sb exists in two crystallographic phases, namely cubic and hexagonal. The cubic phase exhibits a higher quantum efficiency at 532 nm than the hexagonal phase and transforms more easily into CsK_2Sb, tuning this phase is believed to be one of the key parameters in the selective growth of CsK_2Sb.

EXPERIMENTAL

Experiments were performed at the X21 beamline of the National Synchrotron Light Source (NSLS) at Brookhaven National Laboratory and G3 beamline at Cornell Highenergy Synchrotron Source (CHESS), Cornell University. The x-ray beam energy used for the experiments is around 10 keV. The growth experiments were carried out in a UHV system with a $5{\cdot}10^{-10}$ Torr base pressure. Two Pilatus 100k x-ray cameras are mounted outside of the system to record the out-of-plane x-ray diffraction pattern and grazing incidence small angle x-ray scattering GiSAXS data during growth. Besides the diffraction and scatter images, the photocurrent, deposition rate and residual gas composition are recorded. Potassium and Cesium are evaporated from s-shape Alvatec sources. Sb is evaporated from PtSb beads.

Grain sizes were calculated using the well know Scherrer equation.

$$D_{hkl} = \frac{k \cdot \lambda}{B \cdot cos\theta} \quad (1)$$

With λ being the x-ray wavelength, k is the Scherrer constant and taken as 0.9 and B the full width at half maximum (FWHM) in radians and θ the Bragg angle at which the peak is observed.

Sample Preparation and Growth Procedure

As substrate Si(100) is used. The 1 cm x 2 cm samples are cleaned as followed: 10 min in Aceton, rinsing with Isopropanol, 10 min in Isopropanol, rinsing with Isopropanol and drying on a hot plat at 150°C for 10 min. The samples are covered and moved into a fume hood to perform HF dipping to remove the native Oxide layer. After the HF dipping, the samples are rinsed with di H_2O and than stored in di H_2O. This procedure ensured substrate

ISBN: 978-3-95450-132-8 doi:10.18429/JACoW-IPAC2014-MOPRI018

cleanliness and uniformity, sufficient to grow materials (CsK_2Sb) with a quantum efficiency of 5 % and more at 532 nm following the sequential growth procedure.
For the sequential growth the substrate is usually kept at 100°C and as a first preparation step about 50 Å of Potassium are deposited. After that Antimony films of different thickness, ranging from 50 to 150 Å, are evaporated onto the Si(001). The Antimony films as well as all other intermediate materials are characterized using the aforementioned methods. Following the Sb, Potassium is deposited with rates up to 0.2 Å/s. The deposition is stopped after the photocurrent reached a plateau. To maximize the quantum efficiency Cesium is evaporated as a last step. Cesium is as well evaporated at 0.2 Å/s, deposition is stopped once the photocurrent reaches a plateau. For the superlattice type of growth the procedure of the sequential growth was altered. In general the same steps are used as in the sequential growth, but the layer thickness is smaller. Usually Sb thicknesses of not more than 50 Å are deposited. The growth is stopped at a combined Sb layer thickness of 100 - 150 Å.

RESULTS

K_3Sb Growth

Potassium Antimonide films produced following the aforementioned procedure result usually in a mixture of cubic and hexagonal K_3Sb with varying ratios as well as other stoichiometric phases. In the investigated parameter range for substrate temperature and deposition rate it is not possible to drive the reaction in a certain direction and prepare layers of a uniform cubic or hexagonal K_3Sb phase with a certain preferred orientation.

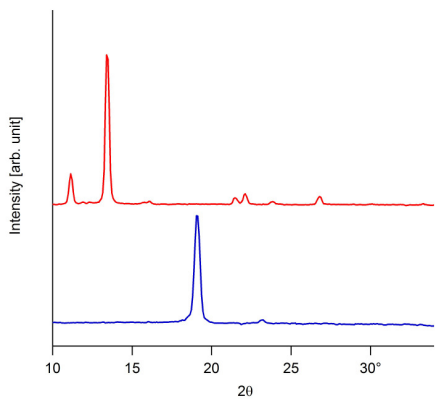

Figure 1: Sequential K_3Sb growth; blue - Sb layer and red - K_3Sb layer.

Fig. 1 shows a typical sequence, with the blue curve for the 100 Å crystalline Sb layer with (003) preferred orientation. The K_3Sb phase is dominantly hexagonal with the most intense Bragg peak at 2θ 13.4° for the (002) orientation. Besides the hexagonal phase this layer exhibits a small contribution of KSb.

Figure 2 shows a typical peak evolution upon K deposition onto a predeposited Sb layer for a cathode grown at a 100°C substrate temperature. K is deposited in 100 Å steps. First a K-Sb phase is built up, followed by the formation of the cubic K_3Sb phase after adding 700 Å of Potassium. Depositing more Potassium leads to the formation of hexagonal K_3Sb at the expense of the cubic K_3Sb phase. Usually at the point of hexagonal K_3Sb formation the photocurrent begins to drop. The layers produced in the sequential growth mode usually are quite rough, with varying quantum efficiency ranging from 0.1 to 0.8% for 532 nm.

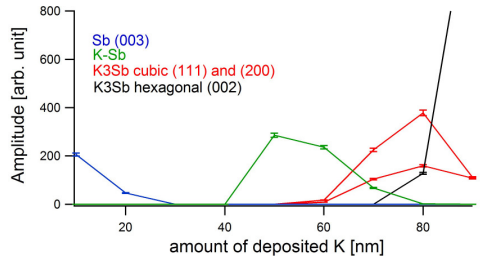

Figure 2: Bragg peak intensity evolution upon K deposition on a predeposited Sb film at a substrate temperature of 100°C. Blue - Sb; green - KSb; red - cubic K_3Sb; black - hexagonal K_3Sb.

To address the roughness a superlattice type of growth was evaluated. Figure 3 shows XRD measurements four of consecutive depositions. Not only did this method yielded quantum efficiencies higher than measured for K-Sb layers following the sequential growth, it also resulted in smoother surfaces. In Figure 3 the corresponding quantum efficiency values for 532 nm displayed on the right. The layers mostly consist of a cubic and hexagonal K_3Sb mixture. The bottom two layers are predominantly cubic K_3Sb with the most intense Bragg peak of the (200) plane at 2θ 17.2°. The top two layers are predominantly hexagonal K_3Sb with the most intense peak for the (002) plane at 2θ 13.6°.

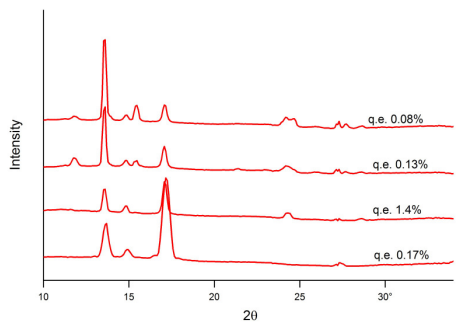

Figure 3: Superlattice type of K_3Sb growth; quantum efficiency values for each step indicated on the right side. The scans are offset for clarity, the bottom being after the first and the top after the fourth deposition. The measurements are taken at 9.7 keV x-ray beam energy.

ISBN: 978-3-95450-132-8 doi:10.18429/JACoW-IPAC2014-MOPRI018

The superlattice type grown layers exhibit a lower roughness compared to layers prepared by the sequential growth mode of similar thickness.

Interaction of K_3Sb modifications with Cs

As a last step in the sequential growth the K_3Sb phase interacts with Cs to form CsK_2Sb. Figure 4 shows all 3 stages of a sequential growth, starting with Sb (blue), K_3Sb (red) and CsK_2Sb (black). It needs to be mentioned that the conversion is not complete in this sample, the Bragg peak of the hexagonal K_3Sb phase at 2θ 13.4° is still distinct. Cs was added in 100 Å steps to monitor the conversion and figure 5 shows the change in the amplitude of the Bragg peaks versus the number of Cs depositions. In total 700 Å of Cs were deposited. It is obvious that the cubic K_3Sb structure (green) can not be resolved after 200 Å of Cs were deposited and the signal for the (200) Bragg peak starts to increase. There is only a slight shift from the Bragg peak originating from the K_3Sb (200) plane to the Bragg peak of the (200) plane of the CsK_2Sb, resulting in an intensity with a nonzero value for the cubic CsK_2Sb structure intensity before Cs is deposited.

From figure 5 it is evident that Cs reacts first with the cubic K_3Sb structure, whereas the hexagonal phase hardly changes upon Cs deposition for the first Cs depositions. Only after the cubic K_3Sb modification is transformed the hexagonal K_3Sb phase interacts slowly with Cesium forming CsK_2Sb.

Table 1: Collection of film thickness, roughness and grain size of every step of the sequentially grown cathode shown in fig. 1. Thickness and roughness values are calculated from corresponding XRR data. All given values are in Å.

Growth Step	Thickness	Roughness	Grain Size
Sb	210.8	9.2	163.6
K-Sb phase	463.8	27.0	
hexagonal K_3Sb			230.6
KSb			248.5
CsK_2Sb	834.6	35.8	134.3

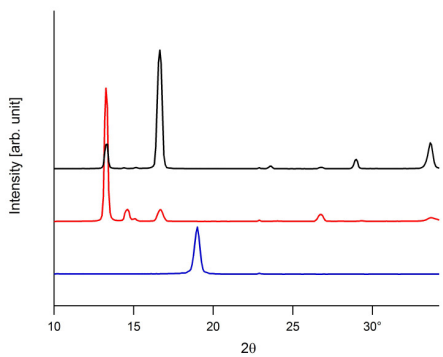

Figure 4: XRD data of a CsK_2Sb sequential growth at 100°C. Blue - Sb, red - K_3Sb and black - CsK_2Sb.

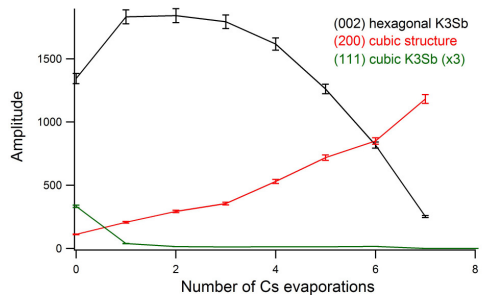

Figure 5: Change of amplitude of (111) cubic K_3Sb (green), (002) hexagonal K_3Sb (black) and (200) cubic CsK_2Sb Bragg peak upon Cs deposition onto K_3Sb cubic/ hexagonal mixture.

SUMMARY

K_3Sb and CsK_2Sb growth studies have been performed using various x-ray diffraction and scattering techniques. Following the sequential growth mode usually results in the formation of a mixture of K_3Sb modifications of varying ratio. These layers are very rough and exhibit quantum efficiencies around 0.1- 0.8 % at 532 nm.

K_3Sb was also formed following a more superlattice type of growth procedure, these films can show a higher quantum efficiency, up to 1.4 % at 532 nm were measured and are smoother than K_3Sb layers of similar thickness prepared by sequential growth.

In a following step the interaction of Cs with a cubic/hexagonal K_3Sb mixture was evaluated. The data gives rise to the assumption that the transformation of the hexagonal K_3Sb phase only occurs once the cubic phase is converted, giving insight to an interesting reaction path.

ACKNOWLEDGMENT

Special thanks to Arthur Woll of G3 beamline at CHESS for his outstanding support and John Walsh for excellent technical work and assistance with the deposition system.

REFERENCES

[1] A. H. Sommer, *Photoemissive Materials*, (Huntington, New York: Robert E. Krieger Publishing Company, 1980).

[2] J. Smedley et al., " Alkali Antimonide Cathodes in a Can", IPAC'14, Dresden, Germany, June 2014, MOPRI063, These Proceedings.

[3] T. Vecchione et al., "Effect of Roughness on Emittance of Potassium Cesium Antimonide Photocathodes", IPAC'12, New Orleans, USA, Proceedings of IPAC2012, 655 (2012).

[4] J. Sangster, A. D. Pelton, Journal of Phase Equilibria 14, 510 (1993).